Bioorganic & Medicinal Chemistry 19 (2011) 5771–5775

Contents lists available at SciVerse ScienceDirect

Bioorganic & Medicinal Chemistry

journal homepage: www.elsevier.com/locate/bmc

A ribonucleopeptide module for effective conversion of an RNA aptamer to a fluorescent sensor

Fong Fong Liew [a], Hironori Hayashi [a], Shun Nakano [a,b], Eiji Nakata [a,b], Takashi Morii [a,b,*]

[a] Institute of Advanced Energy, Kyoto University, Uji, Kyoto 611-0011, Japan
[b] CREST, JST, Uji, Kyoto 611-0011, Japan

ARTICLE INFO

Article history:
Received 1 August 2011
Accepted 12 August 2011
Available online 22 August 2011

Keywords:
Ribonucleopeptide
Biosensor
Modular design
Fluorescent sensor
Aptamer

ABSTRACT

Ribonucleopeptide (RNP) is a new class of scaffold for modular fluorescent sensors. We report here a short RNA motif that induces an efficient communication between the structural changes associated with the ligand-binding event of RNA aptamer and an optical response of a fluorescent RNP module. An optimized short RNA motif was used as a communication module for the rational design of modular RNP sensors. A modular combination of a GTP-binding RNA aptamer, the short RNA motif and the fluorophore-labeled RNP module afforded a fluorescent GTP sensor that retain the ligand-binding affinity of the parent aptamer.

1. Introduction

Optical biosensors for biologically important targets have been developed for various applications in the fields of therapeutics and diagnostics.[1–8] The strategy has successfully provided various biosensors, but it usually requires the lengthy and laborious trial-and-error to obtain a sensor with optimized function. This is because the interplay between the molecular recognition event and the signal-transduction function is unique to the individually constructed biosensor. A modular strategy that permits facile preparation of biosensors with tailored characteristics by a simple combination of a receptor and a signal transducer would accelerate versatile design of optical sensors.[9–12] A few examples of modular aptamer sensors have been reported by fusing two aptamers, one for the target recognition and another for holding a reporter dye, through a connecting stem.[13,14] The strategy provided a modular aptameric sensor with an impressive optical response, but the target affinity of the original aptamer is not always retained in the modular sensors in a predictable manner.

An assembly of RNA and a peptide, such as in the case of RNP (ribonucleopeptide), is a new scaffold for the construction of modular sensors. A stable RNP scaffold was designed by using a complex between RRE (Rev Responsive Element) RNA and a Rev peptide.[15] A randomized nucleotide sequence was introduced into the RNA subunit to construct an RNP library onto which the in vitro selection or SELEX method[16,17] was applied.[18–24] Complex formation of a fluorophore-labeled Rev peptide and the RNA subunit of ATP-binding RNP generates a fluorescent RNP sensor, which enables detection of ATP at tunable wavelengths and/or at a concentration range of interest.[21] The combinatorial approach using RNP thus affords a tailored optical sensor for a given target,[22–24] but the rational design of an optical biosensor from an aptamer remains to be a challenging task. Based on the modularity of the fluorescent RNP sensors, we have recently reported that a simple conjugation of a foreign RNA aptamer and RRE RNA, and successive complex formation with a fluorophore-modified Rev peptide provides a fluorescent RNP sensor.[25] The structural changes associated with substrate binding in the RNA aptamer have been successfully transduced into changes in the fluorescence intensity, though the ratio of fluorescence changes remains to be improved.

In the case for construction of allosteric ribozymes, a short RNA motif termed as a communication module, which connects a ribozyme module and an allosteric ligand-binding module, has been introduced to effectively transduce the structural change associated with the ligand-binding to the ribozyme module.[26] Such a short RNA motif would also be effective for the construction of modular fluorescent RNP sensors. We report here a new modular component to construct fluorescent RNP sensors from the known RNA aptamers. A short RNA motif was introduced that induces an effective communication between a ligand-binding event of RNA aptamer and an optical response of fluorescent RNP. Modular construction with a GTP-binding RNA aptamer, the short RNA motif and the fluorophore-labeled Rev/RRE RNA complex affords a fluorescent GTP sensor that retains the affinity of the parent aptamer.

* Corresponding author. Fax: +81 774 38 3516.
E-mail address: t-morii@iae.kyoto-u.ac.jp (T. Morii).

0968-0896/$ - see front matter © 2011 Elsevier Ltd. All rights reserved.
doi:10.1016/j.bmc.2011.08.031

2. Results and discussion

2.1. Classification of ATP binding RNA by the secondary structure of variable region

From the RNP libraries consisting of randomized 30 nucleotides (RREN30) or randomized nucleotides ranging from 7 to 40 (RRENn), we have isolated RNP receptors for ATP (defined the clone name as A[number] and An[number], respectively).[18,27] Analyses of the relationship of the secondary structure of the RNA subunit (Figs. S1 and S2)[28–30] and the fluorescent property of RNP receptors reveal that the appended RNA consists of predominantly two major regions; a possible ATP-binding region containing a consensus sequence and a variable region that connects RRE RNA and the ATP-binding region (Fig. 1a). Based on the secondary structure of the variable region, structures of RNA were classified into three groups. In type 1, RRE RNA was directly connected to the ATP-binding region. In types 2 and 3, RRE RNA was connected by a rigid stem or by a flexible stem with an internal loop, respectively.

Each RNA was converted to a fluorescent ATP sensor by complexation with 7-methoxycoumarin-labeled Rev (7mC-Rev) to analyze its optical behavior upon ATP-binding (Fig. 1b, Table 1).[21,22,27] In most of the cases, the fluorescence emission was quenched upon formation of the RNP complex and was restored by the ATP binding (Fig. 1b). Changes in the fluorescence intensity of RNP upon ATP-binding, namely the ratio I/I_0 of the initial fluorescence intensity (I_0) and the substrate-bound fluorescence intensity (I), were strongly dependent on the degree by which I_0 was quenched. In type 1 RNP, An16/7mC-Rev showed the I/I_0 ratio of 5.2, which was higher than that of An33/7mC-Rev (1.3, Table 1). An16 and An33 differ only in two nucleotides within the ATP binding region (N_{5-7} in Figs. 1a and S2). All of the fluorescent RNPs in type 2 failed to exhibit a measurable fluorescence response because the I_0 values for these RNP were as large as their corresponding I values. As indicated by type 1 RNP, a slight difference in the ATP-binding region dramatically affects the fluorescence quenching efficiency of I_0, which suggests that a quenching factor exists in the ATP-binding region. This consideration is consistent with the fact that the quenching of I_0 becomes less effective when the rigid stem separates the distance between the ATP-binding region and the 7mC-Rev binding site (RRE RNA) as observed for type 2 RNPs. In contrast, all of the type 3 RNP showed higher I/I_0 values than the type 2 RNP mainly due to the low I_0 values of the type 3 RNP. Upon ATP binding, the 7mC-Rev complexed RNP of A23, A30, and A32 bearing the internal loop in the variable region elicited remarkable changes in the fluorescence intensity, the I/I_0 of 11, 4.0 and 2.5, respectively (Table 1). This result suggests that the stem-loop structure of A23, A30, or A32 is responsible for an alternative quenching mechanism that would be independent of the fluorescence quenching caused by the ATP-binding region as observed for type 1 RNPs. The stem-loop region found in

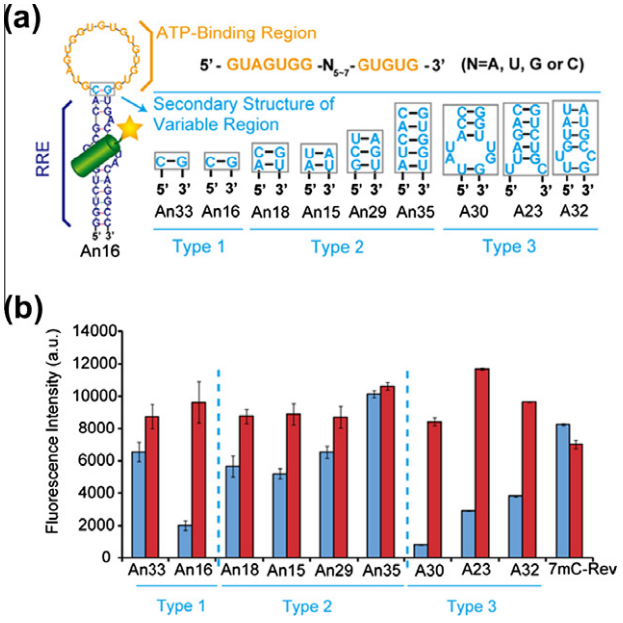

Figure 1. (a) Possible secondary structures of ATP-binding RNPs. (b) Fluorescence intensity of type 1, type 2 and type 3 RNP complexes formed by the indicated RNA subunit and 7mC-Rev, and 7mC-Rev alone are shown in the bar graph. Blue bars and red bars represent the fluorescence intensity in the absence of ATP (I_0) and in the presence of 1 mM ATP (I), respectively.

Table 1
Summary of K_D (μM) and the relative fluorescence intensity ratio (I/I_o) for the ATP binding complex of 7mC-Rev/RNP

RNA variants	An33	An16	An18	An15	An29	An35	A30	A23	A32
K_D (μM)	6.6	1.9	<0.5	<0.5	<0.5	–	8.7	5.8	5.1
I/I_o	1.3	5.2	1.6	1.7	1.4	1.1	11	4.0	2.5

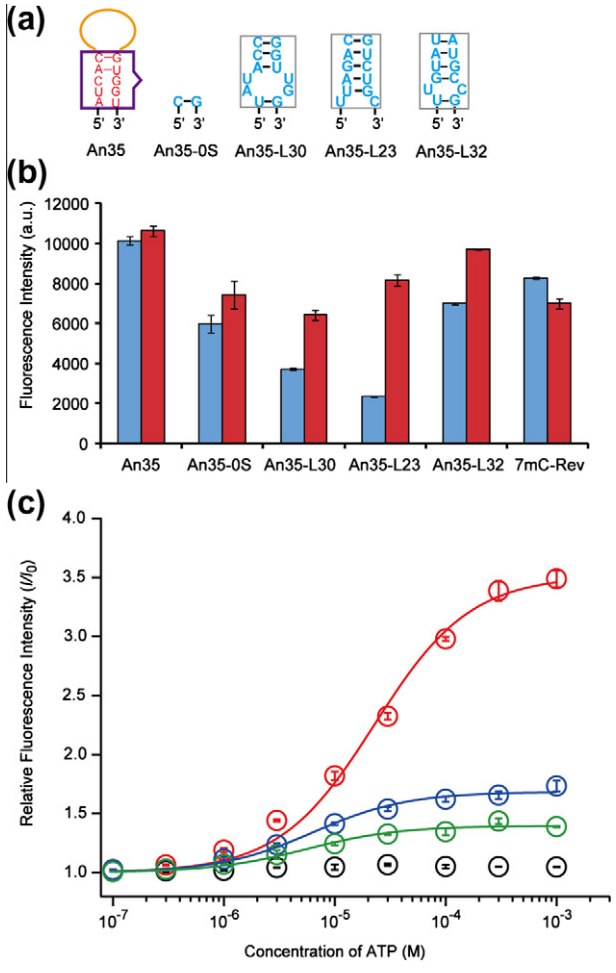

Figure 2. (a) Possible RNA secondary structures of An35, An35-L30, An35-L23 and An35-L32. (b) Fluorescence intensities for RNP of An35 variants and 7mC-Rev and 7mC-Rev alone are shown in the bar graph. Blue bars and red bars represent the fluorescence intensity in the absence of ATP (I_0) and in the presence of 1 mM ATP (I), respectively. (c) Titration curves for the changes in relative fluorescence intensity of An35 (black circles), An35-L23 (red circles), An35-L30 (blue circles) and An35-L32 (green circles) complexed with 7mC-Rev by ATP in 10 mM Tris–HCl (pH 7.6), 100 mM NaCl, 10 mM $MgCl_2$, and 0.005% Tween 20 at 4 °C.

type 3 RNP is then an attractive candidate for a structural motif that controls the degree of fluorescence quenching in accordance with the structural change of the ATP-binding region.

2.2. Validation of the stem-loop motif by evaluation of An35 RNA mutants

In order to validate modularity of the stem-loop motif, mutants of An35 possessing the same sequence in the ATP-binding region were constructed (Fig. 2a). An35 and 7mC-Rev formed a fluorescent RNP with little fluorescence response to ATP (I/I_0 = 1.1). A stem-deleted mutant of An35 (An35-0S/7mC-Rev), which reveals the same secondary structure as type 1 RNP, also shows little fluorescence response (I/I_0 = 1.3). The result indicates that the ATP-binding region of An35 does not contribute to the fluorescence quenching of I_0. Replacing the stem region of An35 with the stem-loop motif derived from A23, A30, or A32 afforded An35-L23, An35-L30 or An35-L32, respectively (Figs. 2 and S3). The ratio I/I_0 of An35-L23/7mC-Rev was improved to 3.5 with K_D of 23 μM, indicating that the stem-loop motif L23 effectively transduced the ATP binding to changes in the emission of 7mC-Rev (Fig. 2 and Table 2). In addition, I/I_0 of An35-L30/7mC-Rev and An35-L32/7mC-Rev were 1.7 and 1.4, respectively, which were also higher than that of parent An35/7mC-Rev.

Table 2
Summary of K_D (μM) and the relative fluorescence intensity ratio (I/I_o) for the ATP binding complex of An35 variants RNP with 7mC-Rev

RNA variants	An35	An35-0S	An35-L23	An35-L30	An35-L32
K_D (μM)	—	6.7	23	6.1	12
I/I_o	1.1	1.3	3.5	1.7	1.4

2.3. Improvement of the stem-loop motif by evaluation of A23 and A30 RNA mutants

Mutants of A23 and A30 at the stem-loop motif were next constructed to improve the efficiency of signal transduction (Figs. 3 and 4, Table 3). Replacing UG adjacent to the loop of A30 to GU (A30GU, Figs. 3a and S4) reduced I/I_0 to 3.1 without significantly losing the binding affinity (K_D = 4.8 μM). A30GC that replaced the UG pair to a U/C mismatch exhibited a large I/I_0 value of 15, but revealed a drastically reduced binding affinity (K_D = 130 μM).

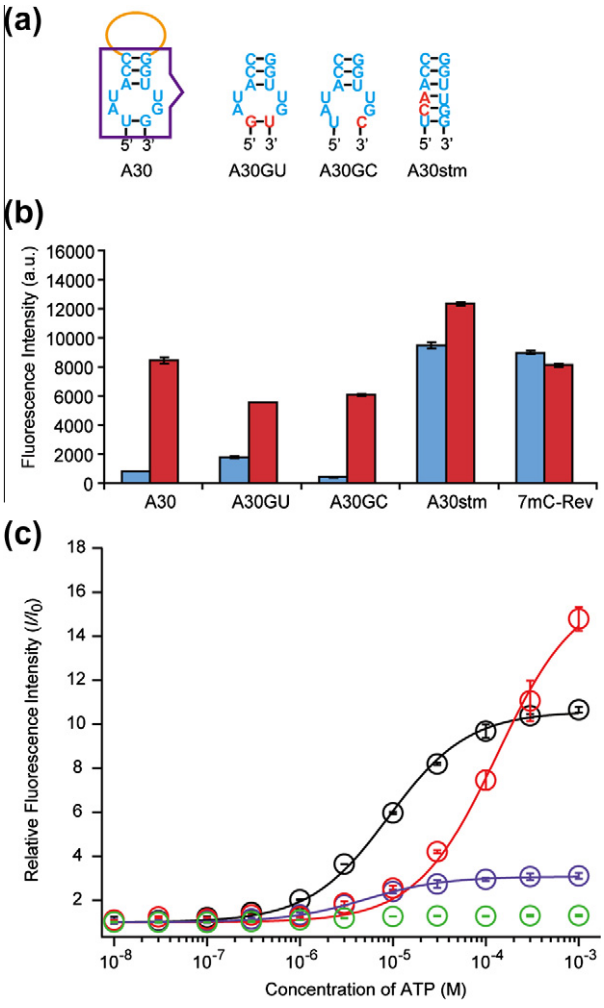

Figure 3. (a) Possible RNA secondary structures of A30 variants. (b) Fluorescence intensities for RNP of A30 variants and 7mC-Rev and 7mC-Rev alone are shown in the bar graph. Blue bars and red bars represent the fluorescence intensity in the absence of ATP (I_0) and in the presence of 1 mM ATP (I), respectively. (c) Titration curves for the relative fluorescent intensity changes of 7mC-Rev complexed A30 (black circles), A30GU (magenta circles), A30GC (red circles) and A30stm (green circles) in 10 mM Tris–HCl (pH 7.6), 100 mM NaCl, 10 mM $MgCl_2$, and 0.005% Tween 20 at 4 °C.

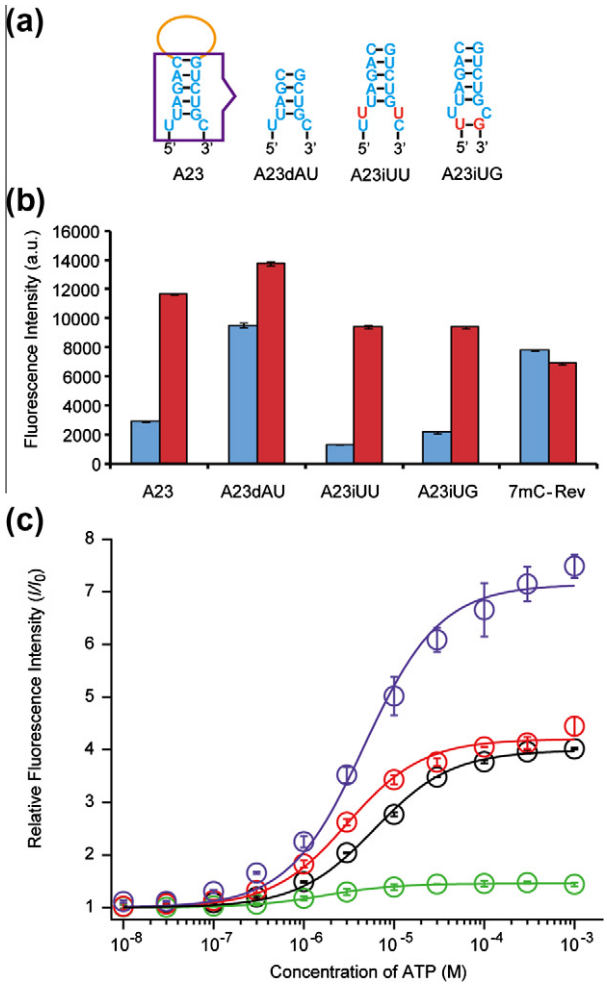

Figure 4. (a) Possible RNA secondary structures of A23 variants. (b) Fluorescence intensities for RNP of A23 variants and 7mC-Rev and 7mC-Rev alone are shown in the bar graph. Blue bars and red bars represent the fluorescence intensity in the absence of ATP (I_0) and in the presence of 1 mM ATP (I), respectively. (c) Titration curves for the relative fluorescent intensity changes of 7mC-Rev complexed A23 (black circles), A23iUG (red circles), A23iUU (magenta circles), A23dAU (green circles) and in 10 mM Tris–HCl (pH 7.6), 100 mM NaCl, 10 mM $MgCl_2$, and 0.005% Tween 20 at 4 °C.

Table 3
Summary of K_D (μM) and the relative fluorescence intensity ratio (I/I_o) for the ATP binding complex of A30 and A23 variants RNPs with 7mC-Rev

RNA variants	A30	A30GU	A30GC	A30stm	A23	A23dAU	A23iUU	A23iUG
K_D (μM)	8.7	48	130	—	5.8	1.4	4.4	2.8
I/I_o	11	3.1	15	1.3	4.0	1.4	7.5	4.4

Table 4
Summary of K_D (μM) and the relative fluorescence intensity ratio (I/I_o) for the GTP binding complex of GTP aptamer variants RNP with 7mC-Rev (4 °C)

RNA variants	GTP-S	GTP	GTP-L23	GTP-L30	GTP-L23iUU	GTP-L23iUG
K_D (μM)	—	<0.5	<0.5	1.6	<0.5	<0.5
I/I_o	1.1	1.8	1.7	2.2	2.9	1.6

In the case of A23 (Figs. 4 and S5, Table 3), deletion of an AU base pair in the stem (A23dAU) retained the affinity to ATP K_D = 1.4 μM), however, it significantly reduced I/I_0 to 1.4. This result indicates that the original stem length of A23 is required to realize the high I/I_0 value. Mutations of the internal loop of A30 indicated that the mismatched U/U pair in the internal loop and the U/G pair adjacent to the internal loop would play important roles in controlling the emission of fluorophore. This idea prompted modifications of A23 by insertion of a U/U mismatch (A23iUU) or a U/G pair (A23iUG) within the stem-loop motif (Fig. 4 and Table 3). As anticipated, A23iUU/7mC-Rev showed an improved I/I_0 ratio of 7.5 (K_D = 4.4 μM) as compared to A23/7mC-Rev (I/I_0 = 4.0; K_D = 5.8 μM) without sacrificing the affinity to ATP. These results indicate that the stem-loop structure of A23, A23iUU, A23iUG or A30 would facilitate a communication between an aptamer binding event and the emission of a fluorophore-labeled Rev peptide in a modular construct of RNP.

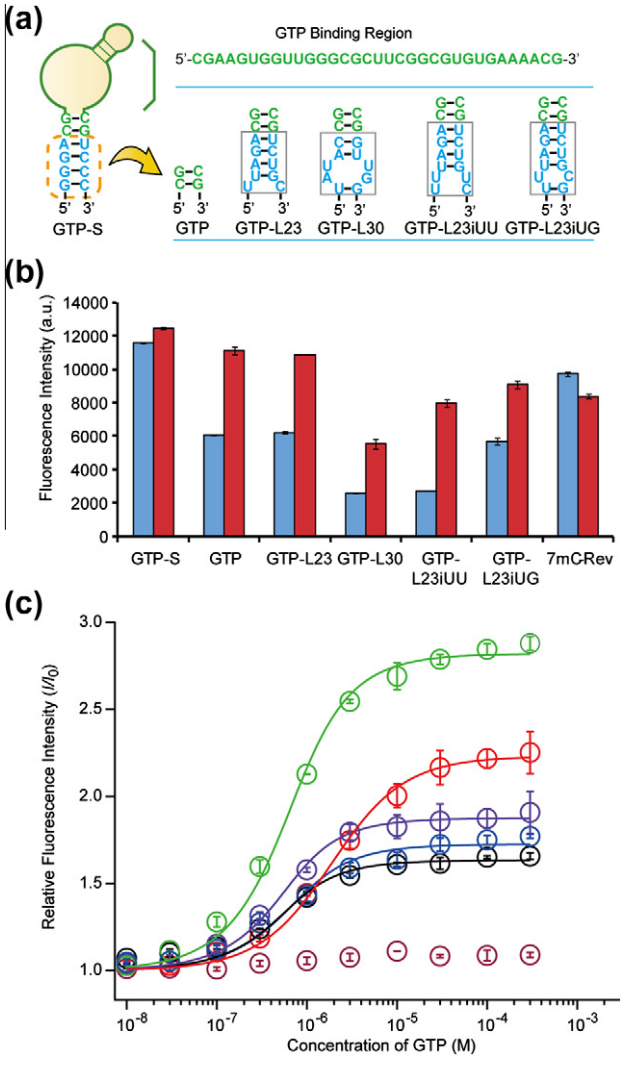

Figure 5. (a) Nucleotide sequences of the stem-loop motif introduced between the GTP aptamer and RRE RNA. (b) Fluorescence intensity of each RNP complex formed by the RNA subunit and 7mC-Rev and 7mC-Rev alone are shown in the bar graph. Blue bars and red bars represent the fluorescence intensity in the absence of GTP (I_0) and in the presence of 1 mM GTP (I), respectively, in 10 mM potassium phosphate (pH 6.2), 200 mM KCl, 2 mM $MgCl_2$, 0.1 mM EDTA and 0.005% Tween 20 at 4 °C. (c) Titration curves for the relative fluorescence intensity changes of 7mC-Rev complexed GTP-S (brown circles), GTP-L30 (red circles), GTP-L23 (blue circles), GTP (purple circles), GTP-L23iUU (green circles) and GTP-L23iUG (black circles) by GTP in 10 mM potassium phosphate (pH 6.2), 200 mM KCl, 2 mM $MgCl_2$, 0.1 mM EDTA and 0.005% Tween 20 at 4 °C.

2.4. Expansion of the stem-loop motifs toward design for effective GTP sensor

In a proof-of-principle experiment, a GTP-binding RNA aptamer reported by Davis et al.[31–33] was conjugated to RRE RNA with or without the stem-loop motif (Figs. 5 and S6). The substrate-binding region of GTP aptamer was first appended directly to RRE RNA and complexed with 7mC-Rev. The resulting construct GTP-S/7mC-Rev exhibited a low I/I_0 of 1.1. The ratio I/I_0 of the stem-deleted mutant (GTP/7mC-Rev) was improved to 1.8. We next introduced the stem-loop structure of A23 RNA (L23), A30 RNA (L30), A23iUU RNA (L23iUU) or A23iUG RNA (L23iUG) between the GTP aptamer and RRE RNA (Fig. 5a). Incorporation of the stem-loop motif L23iUU or L23iUG resulted I/I_0 values of 2.9 and 1.6, respectively, at 4 °C without greatly reducing the GTP binding of original GTP aptamer (Table 4).[31–33] Insertion of the stem-loop motif does not reduce the binding affinity of the fluorescent GTP-binding RNP. This is also the case at the ambient temperature (Table S1). Because the fluorescent GTP-binding RNP bearing the stem region between the GTP aptamer region and RRE RNA (GTP-S/7mC-Rev) failed to exhibit a measurable fluorescence response, the stem-loop motif would be responsible for the observed optical response of the modular GTP sensor.

3. Conclusion

In summary, short RNA stem-loop motifs were identified to effectively transduce the binding event of RNA aptamer to changes in the fluorescence emission at the reporter module, a fluorophore-modified Rev/RRE RNA complex, without a drastic loss of the intrinsic affinity of the aptamer. In principle, the fluorophore at the Rev peptide reporter is changeable as has been previously described, and the aptamer module would be applicable to at least for those under go structural changes in the ligand binding event.[21,23,25] Although the exact mechanism for the quenching and the recovery of fluorescence intensity is yet to be established, the modular strategy described here offers a new root for the rational design of fluorescent biosensors from RNA aptamers.

4. Materials and methods

ATP (adenosine triphosphate) and GTP (guanosine triphosphate) were purchased from Sigma-Aldrich. *N*-Fmoc-protected amino acids, HBTU (2-(1*H*benzotriazole-1-yl)-1,1,3,3-tetramethyl uronium hexafluorophosphate), 1-hydroxybenzotriazole (HOBt), DIEA (*N*,*N*-diisopropylethylamine), TFA (trifluoroacetic acid), and distilled DMF (*N*,*N*-dimethylformamide) were obtained from Watanabe Chemical Industry. Fmoc-PAL-PEG resin (0.38 mmol/g)

was purchased from Applied Biosystems. Gel electrophoresis grade acrylamide and bisacrylamide were obtained from Wako Chemicals. All other chemicals were reagent grade and used without further purification. The Rev peptide modified with 7-methoxycoumarin-3-carboxylic acid (7mC-Rev) was synthesized as described previously

4.1. Nucleic acids preparations

The nucleic acids used in this study were prepared according to the procedure previously reported.[18,27] Concentration of RNA was determined by UV spectroscopy.

4.2. 7mC-Rev peptide preparation

The procedure for the synthesis of fluorophore-labeled Rev peptides were previously reported.[21] Briefly, the Rev peptide was synthesized on a Shimadzu PSSM-8 peptide synthesizer according to the Fmoc chemistry protocols. The fluorophore 7mC with an activated group was directly coupled to the N-terminal deprotected Rev peptide on the resin. The 7mC-labeled peptide-resin was then deprotected and cleaved from resin and purified by using gel filtration and RP-HPLC, and characterized by MALDI-TOF MS spectrometry (AXIMA-LNR, Shimadzu Biotech) $[7mC\text{-}Rev+H]^+$ calc. m/z 2638.44, obs. m/z 2638.29.

4.3. Analysis of secondary structures

Secondary structures of the RNA subunits of RNP used in this study were analyzed by mfold version 3.2 (http://mfold.rna.albany.edu/). Folding was done at 37 °C with 1 M NaCl, specifying that the RRE region is in the reported secondary structure.[28–30]

4.4. Fluorescence measurements on the microplate

The 96-well fluorescence measurements were performed on a Wallac ARVOsx 1420 multilabel counter. For the ATP titration, a binding solution (100 μL) containing 0.5 μM of fluorescent RNP in 10 mM Tris–HCl (pH 7.6), 100 mM NaCl, 10 mM $MgCl_2$, 0.005% Tween 20 was prepared. For the GTP titration, a binding solution (100 μL) containing 0.5 μM of fluorescent RNP in 10 mM potassium phosphate (pH 6.2), 200 mM KCl, 2 mM $MgCl_2$, 0.1 mM EDTA and 0.005% Tween 20 were prepared. Well-mixed samples with the different concentration of substrate (ATP or GTP) were incubated at 4 °C or 25 °C for 30 min followed by the measurement of emission spectra. Excitation and emission wavelengths were measured at λ_{ex} = 355 nm, and λ_{em} = 390 nm, respectively.

4.5. Determination of binding affinity

The binding affinity of fluorescent RNP was obtained by fitting the substrate titration data using the equation:

$$\text{Fobs} = A\{([\text{FRNP}]_T + [\text{substrate}]_T + K_D) - \{([\text{FRNP}]_T + [\text{substrate}]_T + K_D)^2 - 4[\text{FRNP}]_T[\text{substrate}]_T\}^{1/2}\}/2[\text{FRNP}]_T$$

Where A is the increase in fluorescence at saturating substrate concentrations ($F_{max} - F_{min}$), K_D is the dissociation constant, and $[FRNP]_T$ and $[substrate]_T$ are the total concentration of fluorescent RNP and the substrate (ATP or GTP), respectively.

Acknowledgment

This work was supported in part by Grants-in-Aid for Scientific Research from the Ministry of Education, Culture, Sports, Science and Technology, Japan to T.M. (Nos. 20241051 & 22121510).

Supplementary data

Supplementary data (Nucleotide sequence and secondary structure of RNA subunit of ATP binding RNP obtained from RRENn library and RREN30 library (Figures S1 and S2), An35 variants (Figure S3), A30 variants (Figure S4), A23 variants (Figure S5) and GTP RNA variants (Figure S6), binding characteristic of GTP RNA variants at 25 °C (Table S1)) associated with this article can be found, in the online version, at doi:10.1016/j.bmc.2011.08.031.

References and notes

1. Giepmans, B. N. G.; Adams, S. R.; Ellisman, M. H.; Tsien, R. Y. *Science* **2006**, *312*, 217.
2. Johnsson, N.; Johnsson, K. *ACS Chem. Biol.* **2007**, *2*, 31.
3. Famulok, M.; Hartig, J. S.; Mayer, G. *Chem. Rev.* **2007**, *107*, 3715.
4. Lavis, L. D.; Raines, R. T. *ACS Chem. Biol.* **2008**, *3*, 142.
5. Wang, H.; Nakata, E.; Hamachi, I. *ChemBioChem* **2009**, *10*, 2560.
6. Cho, E. J.; Lee, J.-W.; Ellington, A. D. *Annu. Rev. Anal. Chem.* **2009**, *2*, 241.
7. Tainaka, K.; Sakaguchi, R.; Hayashi, H.; Nakano, S.; Liew, F. F.; Morii, T. *Sensors* **2010**, *9*, 1355.
8. Han, K.; Liang, Z.; Zhou, N. *Sensors* **2010**, *10*, 4541.
9. Breaker, R. R. *Curr. Opin. Biotechnol.* **2002**, *13*, 31.
10. Silverman, S. K. *RNA* **2003**, *9*, 377.
11. Famulok, M. *Curr. Opin. Mol. Ther.* **2005**, *7*, 137.
12. Navani, N. K.; Li, Y. *Curr. Opin. Chem. Biol.* **2006**, *10*, 272.
13. Stojanovic, M. N.; Kolpashchikov, D. M. *J. Am. Chem. Soc.* **2004**, *126*, 9266.
14. Furutani, C.; Shinomiya, K.; Aoyama, Y.; Yamada, K.; Sando, S. *Mol. BioSyst.* **2010**, *6*, 1569.
15. Battiste, J. L.; Mao, H.; Rao, N. S.; Tan, R.; Muhandiram, D. R.; Kay, L. E.; Frankel, A. D.; Williamson, J. R. *Science* **1996**, *273*, 1547.
16. Ellington, A. D.; Szostak, J. W. *Nature* **1990**, *346*, 818.
17. Tuerk, C.; Gold, L. *Science* **1990**, *249*, 505.
18. Morii, T.; Hagihara, M.; Sato, S.; Makino, K. *J. Am. Chem. Soc.* **2002**, *124*, 4617.
19. Sato, S.; Fukuda, M.; Hagihara, M.; Tanabe, Y.; Ohkubo, K.; Morii, T. *J. Am. Chem. Soc.* **2005**, *127*, 30.
20. Hasegawa, T.; Ohkubo, K.; Yoshikawa, S.; Morii, T. *E-J. Surf. Sci. Nanotechnol.* **2005**, *3*, 33.
21. Hagihara, M.; Fukuda, M.; Hasegawa, T.; Morii, T. *J. Am. Chem. Soc.* **2006**, *128*, 12932.
22. Hasegawa, T.; Hagihara, M.; Fukuda, M.; Morii, T. *Nucleosides Nucleotides Nucleic Acids* **2007**, *26*, 1277.
23. Hasegawa, T.; Hagihara, M.; Fukuda, M.; Nakano, S.; Fujieda, N.; Morii, T. *J. Am. Chem. Soc.* **2008**, *130*, 8804.
24. Liew, F. F.; Hasegawa, T.; Fukuda, M.; Nakata, E.; Morii, T. *Bioorg. Med. Chem.* **2011**, *19*, 4473.
25. Nakano, N.; Nakata, E.; Morii, T. *Bioorg. Med. Chem. Lett.* **2011**, *21*, 4503.
26. Kertsburg, A.; Soukup, G. A. *Nucleic Acids Res.* **2002**, *30*, 4599.
27. Nakano, S.; Mashima, T.; Matsugami, A.; Inoue, M.; Katahira, M.; Morii, T. *J. Am. Chem. Soc.* **2011**, *133*, 4567.
28. Zuker, M. *Science* **1989**, *244*, 48.
29. Mathew, D. H.; Sabina, J. K.; Zuker, M.; Turner, D. H. *J. Mol. Biol.* **1999**, *288*, 911.
30. Zuker, M. *Nucleic Acids Res.* **2003**, *31*, 3406.
31. Davis, J. H.; Szostak, J. W. *Proc. Natl. Acad. Sci. U.S.A.* **2002**, *99*, 11616.
32. Carothers, J. M.; Oestreich, S. C.; Davis, J. H.; Szostak, J. W. *J. Am. Chem. Soc.* **2004**, *126*, 5130.
33. Carothers, J. M.; Goler, J. A.; Kapoor, Y.; Lara, L.; Keasling, J. D. *Nucleic Acids Res.* **2010**, *38*, 2736.